Research Square

Preprints are preliminary reports that have not undergone peer review.
They should not be considered conclusive, used to inform clinical practice,
or referenced by the media as validated information.

Impact of Micelle-Mediated Mass Transport of Oxidation Products on the Stability of Flaxseed Oil Emulsions

Xintian Wang
Wuhan Textile University
Hongjian Chen
Hubei University
Qian Zhang
Wuhan Textile University
Xingfang Xiao
Wuhan Textile University
Alejandro Cifuentese
Foodomics Laboratory, Institute of Food Science Research (CIAL), CSIC
Elena Ibanezde
Foodomics Laboratory, Institute of Food Science Research (CIAL), CSIC
Bifeng Liu
Huazhong University of Science and Technology
Peiwu Li
Oil Crops Research Institute of Chinese Academy of Agricultural Sciences
Zhaowei Zhang
Wuhan Textile University
Qianchun Deng
dengqianchun@caas.cn

Oil Crops Research Institute of Chinese Academy of Agricultural Sciences

Article

Keywords: flaxseed oil, emulsion, lipid oxidation, micelle, mass transport

Posted Date: November 12th, 2026

DOI: https://doi.org/10.21203/rs.3.rs-11002190/v1

License: This work is licensed under a Creative Commons Attribution 4.0 International License.
Read Full License

Additional Declarations: No competing interests reported.

Impact of Micelle-Mediated Mass Transport of Oxidation Products on the Stability of Flaxseed Oil Emulsions

Xintian Wang[1,2,3], Hongjian Chen[4], Qian Zhang[1], Xingfang Xiao[1], Alejandro Cifuentese[5], Elena Ibanezde[5], Bifeng Liu[3], Peiwu Li[2,6], Zhaowei Zhang[1,2*], Qianchun Deng[2*]

[1.] *School of Biomedical Engineering and Health, State Key Laboratory of New Textile Materials and Advanced Processing Technologies, Hubei Jiangxia Lab, Wuhan Textile University, Wuhan, 430200, China*

[2.] *Oil Crops Research Institute of Chinese Academy of Agricultural Sciences, Wuhan, Hubei 430062, China.*

[3.] *School of Life Science and Technology, Huazhong University of Science and Technology, Wuhan, Hubei 430074, China.*

[4.] *School of Health Science and Engineering, Hubei University, Wuhan, Hubei 430062, China.*

[5.] *Foodomics Laboratory, Institute of Food Science Research (CIAL), CSIC, 28049 Madrid, Spain*

[6.] *Zhejiang Xianghu Laboratory, Hangzhou, 311231, PR China*

*** Corresponding authors:**

Zhaowei Zhang: zwzhang@whu.edu.cn

Qianchun Deng: dengqianchun@caas.cn

Abstract

The physicochemical stability of emulsions is critically influenced by the aqueous phase micelle-mediated dynamic transport of oxidation products. In this study, the dynamic migration of lipid oxidation products was investigated in flaxseed oil emulsions stabilized by five surfactants- Tween 20 (T20), sodium dodecyl sulfate (SDS), cetyltrimethylammonium bromide (CTAB), saponin (QS), and phospholipid (PL). Initial droplet sizes ranged from 0.15 to 0.29 μm, with SDS- and CTAB-stabilized emulsions exhibiting superior physical stability (TSI < 1.5) throughout storage. PL and QS generated highly viscous, polar interfaces that sterically impeded reactant diffusion, restricting aqueous phase lipid hydroperoxide (LOOH) concentrations to 6.56 and 5.50 μmol/L, respectively. Conversely, SDS and CTAB formed low-viscosity, highly fluid films that accelerated mass transport, with CTAB micelles exhibiting a propensity to transfer lower-molecular-weight secondary oxidation products, such as malondialdehyde (MDA, 3.46 μmol/L). Notably, T20 micelles facilitated the partitioning of LOOH into the aqueous phase (up to 23.95 μmol/L), spatially isolating these primary products from the oxidation sites. The above partitioning delayed the further degradation of LOOH, resulting in a slow increase in emulsion TBARS content (0.28-1.32 mmol/kg oil). By correlating interfacial structure with micelle-driven mass transfer, this work provides a theoretical basis for stabilizing flaxseed oil emulsions rich in n-3 polyunsaturated fatty acids.

Keywords: flaxseed oil; emulsion; lipid oxidation; micelle; mass transport

1. Introduction

Flaxseed oil emulsions enriched with α-linolenic acid (ALA) are highly prone to oxidation, which severely hinders nutrient preservation and their application in food supplements. In the preparation of oil-in-water (O/W) emulsions using small molecule surfactants, the surfactant molecules adsorb onto the oil/water interface until saturation, with the excess molecules remaining in the continuous phase. When the concentration exceeds the critical micelle concentration (CMC), micelles spontaneously form in the continuous phase. These surfactant micelles can solubilize small molecules (such as lipid oxidation products and antioxidants) and form mixed micelles with other surface-active compounds[1]. Ultimately, partitioning of emulsion components across the oil, aqueous, and interfacial phases undergoes modification, thereby impacting the pathways and rates of the oxidation reaction[2].

Within heterogeneous systems, the “polar paradox” and “cut-off” effect theories suggest that the localization of antioxidants at the oil-water interface is essential for their effectiveness in inhibiting lipid oxidation[3]. The lipid oxidation of O/W emulsions becomes significantly more complex in the presence of aqueous phase micelles, which function as dynamic delivery platforms facilitating mass exchange between oil droplets[2,4,5]. These micelles are capable of transporting antioxidants from the oil droplet core to the interface, thereby enhancing their efficacy[6]. Concurrently, they can act as carriers for amphiphilic lipid hydroperoxides (LOOH), translocating them from the interface into the aqueous micelles or to adjacent droplets, which ultimately decelerates or accelerates the overall oxidation rate[7,8]. This dual capacity of micelles to deliver both antioxidant and pro-oxidant molecules dictates that their effect-whether pro-oxidative or anti-oxidative-is highly system-dependent. The interfacial physicochemical properties of micelles vary drastically depending on the surfactant type (e.g., ionic or non-ionic), potentially leading to different diffusion behaviors of oxidation products and distinct tendencies to form mixed micelles[8,9]. Therefore, understanding the role of micelles in the dynamic mass exchange of these oxidation products, along with its

subsequent impact on the localization and reactivity of active molecules, is essential for the steady-state regulation of flaxseed oil emulsions.

In this study, the role of micelles in regulating the stability of flaxseed oil emulsions was investigated by formulating emulsions with distinct surfactants, including Tween 20, sodium dodecyl sulfate (SDS), cetyltrimethylammonium bromide (CTAB), quillaja saponin (QS), and phospholipids (PL). This work established a mechanistic link between the macroscopic physicochemical stability of the emulsions and the microscopic behavior of aqueous micelles, specifically focusing on the dynamic mass transport of oxidation products. The intrinsic mechanism by which micelles influence emulsion stability was systematically elucidated from the multidimensional perspectives of the oil, aqueous, micelle, and interfacial phase.

2 Materials and Methods

2.1 Materials

T20, SDS, CTAB, and QS were sourced from Sigma-Aldrich (Saint Louis, MO, USA). PL was obtained from Shanghai Macklin Biochemical Technology Co., Ltd. (Shanghai, China). Analytical grade organic reagents were provided by Sinopharm Chemical Reagent Co., Ltd. (Beijing, China). Triglyceride assay kits, lipid hydroperoxide assay kit and an MDA assay kit and were obtained from Nanjing Jiancheng Bioengineering Institute (Nanjing, China).

2.2 Sample Preparation

Stripped flaxseed oil (SFO) was obtained according to a previous report[10]. O/W emulsions were modified from a previously report[11]. A coarse emulsion was produced by blending 90% (w/w) aqueous phase (containing 2% T20, PL, SDS, CTAB, or QS in pH 7 phosphate buffer) with 10% (w/w) SFO oil phase, using a high-speed shear homogenizer (IKA, Germany) at 10,000 rpm for 2 minutes. Subsequently, the mixture was processed through M-110EH30 high-pressure microfluidizer (Microfluidics, USA) to obtain flaxseed emulsions. The emulsions were stored in a dark, constant temperature and humidity chamber at 37°C, and samples were periodically taken for analysis.

2.3 The Physical Stability of Emulsions

Particle size determination: The average droplet diameter of the prepared emulsions was determined via static light scattering (SLS) using a Mastersizer 3000 instrument (Malvern Instruments, UK)[12].

ζ-potential determination: A Malvern Zetasizer NanoZS (Malvern Instruments, Worcs., UK) was used to measure the ζ-potential of the emulsions based on dynamic light scattering (DLS). Refractive index values of 1.490 for flaxseed oil and 1.330 for the aqueous phase were applied in the measurements[13].

Assessment of physical stability via multiple light scattering: A Turbiscan Lab Expert stability analyzer (Formulation, France) was employed to continuously monitor the physical stability of the emulsions during storage at 37 °C. The Turbiscan Stability Index (TSI) was calculated using the associated Turbiscan Easy Soft software.

Microstructure: Confocal laser scanning microscopy (CLSM, Nikon, Melville, NY) was used to visualize the microstructure of the emulsions. A 1:1 (v/v) mixture of the emulsion and phosphate buffer was stained with Nile red dissolved in ethanol (1 mg/mL). Image analysis was performed with the instrument's built-in software (NIS Elements, Nikon, NY).

2.4 The Chemical Stability of Emulsions

Primary and secondary oxidation products determination: The concentrations of lipid hydroperoxides (LOOH) and thiobarbituric acid reactive substances (TBARS) were measured periodically throughout storage, following the methods described in a prior publication[14]. Results are expressed as millimoles of cumene hydroperoxide equivalents per kg of oil (for LOOH) and as millimoles of 1,1,3,3-tetraethoxypropane (TEP) equivalents per kg of oil (for TBARS).

2.5 Particle Size and Microstructure of Emulsion Aqueous Phase

The emulsion (1 mL) was centrifuged at 27,721 × g for 60 min at 4 °C, and the procedure was carried out in triplicate. The clear lower aqueous layer was collected by making a small puncture at the bottom of the centrifuge tube. Cryo-transmission electron microscope (Cryo-TEM, Glacios 200 kV Thermo Fisher, USA) was used to

examine the morphology of micelle structures. All samples were vitrified on TEM copper grids coated with a holey carbon film[15]. DLS was used to track the evolution of micelle size within the aqueous phase over the storage period.

2.6 Triacylglycerol (TG) Content in Emulsion Aqueous Phase

A commercial colorimetric triglyceride assay kit was used to quantify the TG content in the emulsion aqueous phase. After mixing 2.5 μL of sample (or standard) with 250 μL of working solution, the mixture was incubated at 37 °C for 10 min. A microplate reader was used to record the absorbance at 500 nm against distilled water (blank). TG concentrations were calculated using the equation below:

$$\text{Triglyceride content(mmol/L)}=\frac{A_{sample}-A_{control}}{A_{standard}-A_{control}}\times C_{standard}$$

Where, A_{sample}, $A_{standard}$, and $A_{control}$ represent the absorbances of the sample, standard, and control, respectively.

2.7 Determination of Oxidation Products in Emulsion Aqueous Phase

The concentrations of LOOH and malondialdehyde (MDA) in the emulsion aqueous phase were quantitatively analyzed using a lipid hydroperoxide assay kit and an MDA assay kit, respectively [7].

2.8 Dynamic Interfacial Tension (DIFT) Measurement

The DIFT at the oil-water interface was assessed using the pendant drop protocol of Joshi et al[16]. PBS solution served as the aqueous phase, and SFO was used as the oil phase. The measuring vessel was directly coupled to a syringe fitted with a piston via a threaded connection on a Tracker interfacial rheometer (Teclis, France).

2.9 Determination of Emulsion Interfacial Film Properties

A spin probe method coupled with electron paramagnetic resonance (EPR) spectroscopy was used to characterize the interfacial properties of the O/W emulsions. Measurements were performed on a Bruker A300-10/12 EPR spectrometer (Bruker, Germany) [17,18]. The following instrumental settings were applied for data collection and processing: central magnetic field = 0.349 T, scan width = 0.01 T, gain = 5.64×10^3, and time constant = 5.12 ms.

Samples were prepared as follows: initially, a 7.8 mM stock solution of the spin

probe 5-DSA was prepared in absolute ethanol. Subsequently, stock solution (15μL) was transferred into a test tube. Following ethanol evaporation, 1 mL of the emulsion was added to each tube and maintained at room temperature for 1 day to permit dissolution of the probe into the surfactant layer. The resulting final concentration of 5-DSA in the emulsions was 0.12 mM. Relevant parameters were calculated as follows[19-21]:

Rotational correlation time (τ_R) calculation:

$$\tau_R=\left(6\times10^{-10}\right)\left[(h_0/h_{+1})^{\frac{1}{2}}+(h_0/h_{-1})^{\frac{1}{2}}-2\right]*\Delta H_0$$

where h_{+1}, h_0, and h_{-1} represent the amplitudes of the three hyperfine lines (**Fig. 1**). ΔH_0 is the linewidth of the central line. Alterations in the τ_R value of the 5-DSA reflect the degree of motional restriction experienced by the spin probe within its local microenvironment.

The order parameter (S) calculation:

$$S=(A_{\parallel}-A_{\perp})/[A_{ZZ}-{}^{1}\!/_{2}\,(A_{XX}+A_{YY})]({}^{\alpha_0}\!/_{\alpha_0'})$$

Where, A_{XX}, A_{YY}, A_{ZZ} are the single-crystal values of 5-DSA, equal to 6.3, 5.8, and 33.6 G, respectively. $A_{/\!/}$ corresponds to half the distance of the outer maximum hyperfine splitting. $A_{\perp}$ is calculated according to the following formula:

$$A_{\perp}=A_{min}+1.4(1-S^{app})$$

$$S^{app}={}^{(A_{max}-A_{min})}\!/_{(A_{ZZ}-\frac{1}{2}(A_{XX}+A_{YY}))}$$

Where, A_{min} represents half distance of the inner minimum hyperfine splitting.

The isotropic hyperfine splitting constant α_0 for the nitroxide molecule in its crystalline state is given by:

$$\alpha_0={}^{(A_{ZZ}+A_{XX}+A_{YY})}\!/_{3}$$

and α_0', the corresponding constant for the spin probe, is calculated as

$$\alpha_0'={}^{(A_{\parallel}+2A_{\perp})}\!/_{3}$$

The ratio α_0/α_0' serves as a polarity correction factor (hyperfine splitting constant).

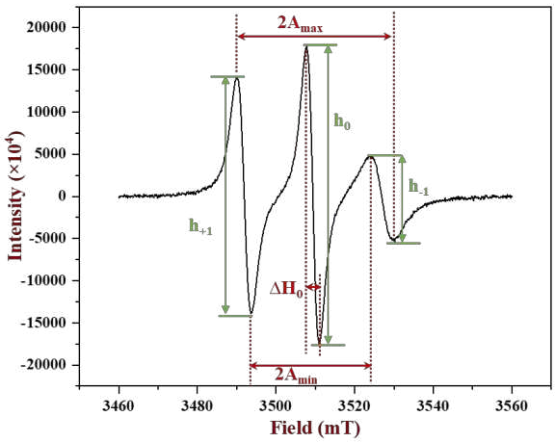


Fig.1 Schematic illustration of the EPR spectrum obtained from the 5-DSA spin probe.

2.10 Data Analysis

All experimental results are expressed as the mean ± standard deviation. Data analysis was carried out using SPSS version 21.0 (SPSS, Inc., Chicago, IL, USA), with statistical significance defined as $P < 0.05$.

3. Results and Discussion

3.1 The Physical Stability of Emulsion

During the storage period, the particle size, ζ-potential, TSI, and microstructure of the various emulsions were evaluated (**Fig. 2**). The initial oil droplets exhibited significant discrepancies in their volume-surface mean diameters (D [3,2], **Fig. 2a**). The emulsions stabilized by T20 and QS displayed comparable initial sizes, with D [3,2] approximating 0.28 - 0.29 μm, whereas the PL-stabilized emulsion exhibited a D [3,2] of 0.22 μm. Emulsions formulated with anionic SDS and cationic CTAB possessed smaller initial particle sizes, with D [3,2] values ranging from 0.15 to 0.16 μm. The initial droplet size was fundamentally governed by the interaction between droplet disruption and aggregation during the microfluidization process. Consequently, the initial droplet size might depend on the surfactant's interfacial adsorption efficiency and emulsifying performance[22,23]. Furthermore, the preferential adsorption of anionic impurities residing within the oil or surfactant phase, alongside hydroxyl ions originating from the aqueous phase, may confer a partial negative charge to the resultant emulsion[24]. Therefore, the initial negative charge of the T20 (a non-ionic surfactant)

emulsion was relatively low (-8.61 mV) and progressively increased to approximately -35 mV during storage (**Fig. 2b**). At pH 7, PC operates as a zwitterionic surfactant characterized by a neutral net charge[25]. The initial negative charge (-7.65 mV) observed on the PL emulsion droplets may be due to the minor alternative constituents within the phospholipid formulation, such as phosphatidylserine and phosphatidylinositol[11,26,27]. Concurrently, throughout the storage duration, the ζ-potential values of the oil droplets grew increasingly negative. This phenomenon may arise from anionic lipid breakdown products (e.g., free fatty acids or organic acids) that gradually change the interfacial composition[28,29]. The initial droplet potentials of the QS and SDS emulsions reached -60 and -80 mV, respectively, while the emulsion droplets stabilized by the cationic CTAB exhibited a ζ-potential of roughly +35 mV, which remained largely unaltered throughout the entire storage period.

As time progressed, the emulsions may have undergone various destabilization pathways. Turbiscan stability index (TSI) serves as a metric to evaluate overall emulsion stability, encompassing processes such as droplet coalescence and sedimentation[30-32]. A lower TSI value inherently corresponds to enhanced emulsion stability[33]. As depicted in **Fig. 2c**, the order of TSI values was QS > T20 > PL > SDS > CTAB. The comparatively elevated storage stability exhibited by SDS and CTAB emulsions was primarily attributable to the fact that the creaming rate scaled with the square of the droplet diameter. Consequently, a reduction in droplet size markedly delayed oil-water segregation. In contrast, the poorer physical stability of QS and T20 emulsions, the partial aggregation phenomenon that occurred after 21 d as shown in **Fig. 2d**, might be due to the insufficient electrostatic repulsion to prevent flocculation. Differences in physical stability across surfactant-stabilized emulsions arose not only from electrostatic effects but also from variations in oxidation kinetics, interfacial barrier properties, and steric hindrance. The distribution of oxidation products within the emulsion dictated the enhancement or deterioration of oxidative stability, which subsequently impacted the physical stability of the system.

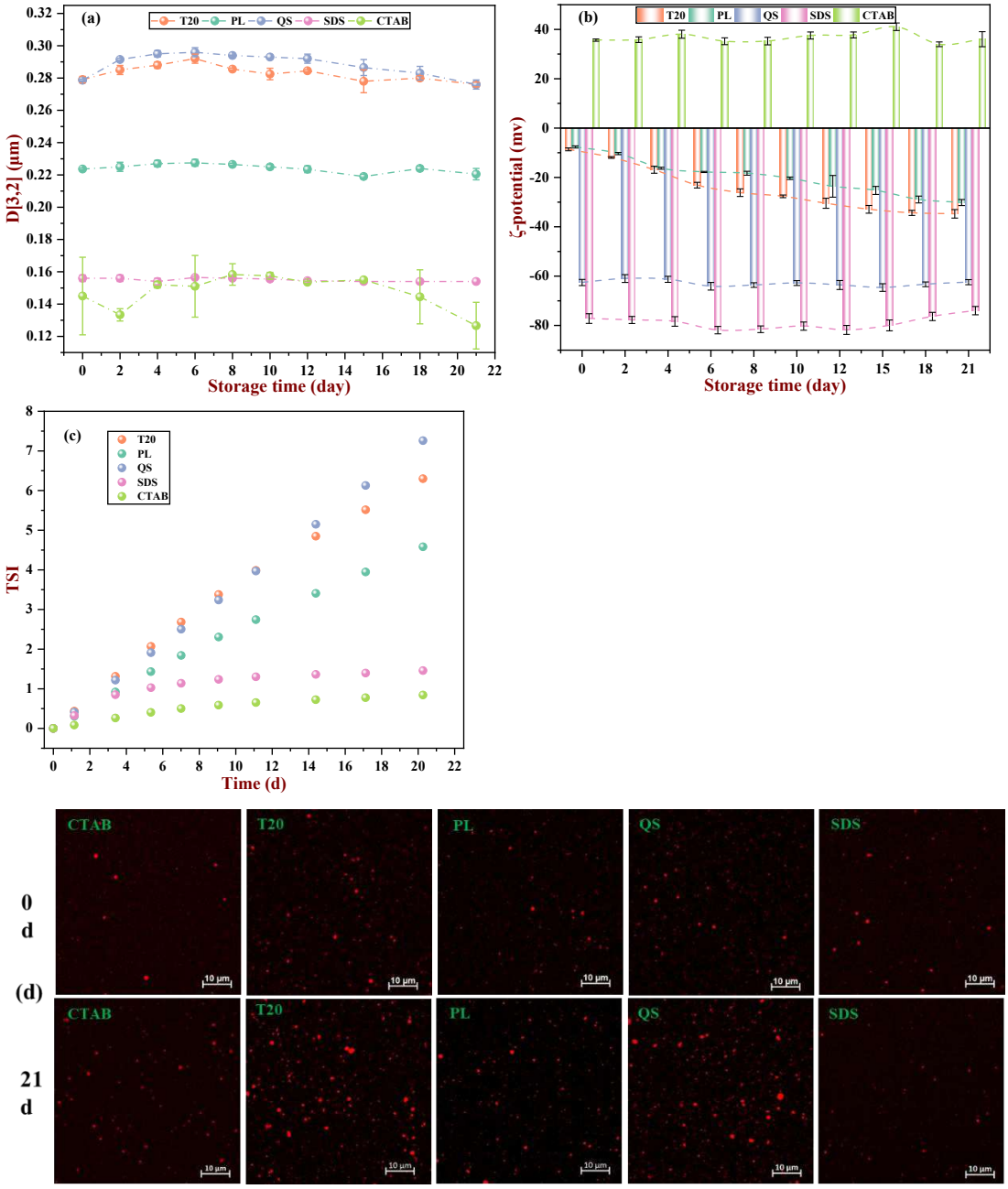


Fig. 2 The changes of the particle diameters D [3,2] (a), ζ-potential (b), TSI (c), and microstructure (d) during the storage of flaxseed oil emulsion

3.2 The Chemical Stability of Emulsion

Oxidative stability was determined from the measured concentrations of primary (LOOH) and secondary (TBARS) oxidation products over the storage time. As showed in **Fig. 3a**, the levels of LOOH within the emulsions increased with prolonged storage time. T20 and SDS did not demonstrate a discernible lag phase, with LOOH concentrations escalating rapidly during the initial stages of storage. Conversely, the

LOOH concentrations for PL and QS experienced an abrupt surge on days 10 (increasing from 0.75 to 1.71 mmol/kg oil) and 15 (increasing from 0.28 to 0.70 mmol/kg oil), respectively. CTAB maintained lower LOOH concentrations (0.26-0.73 mmol/kg oil) throughout the entire storage duration, demonstrating superior chemical stability. The electrostatic repulsion of transition trace metal ions by the positively charged CTAB (+35 mV) likely delayed the oxidation progression. Concurrently, the anionic surfactant SDS yielded the highest TBARS values (10.78 mmol/kg oil), followed by PL, T20, and CTAB ≈ QS (**Fig.3b**). This result may be related to its initially elevated levels of lipid oxidation products. Although T20 had the highest LOOH concentration (5.31 mmol/kg oil), TBARS concentration exhibited a slow growth rate (from 0.28 to 1.32 mmol/kg oil). This phenomenon was potentially attributable to the micelle-mediated transport of LOOH from the oil phase to the aqueous phase, which spatially separated these primary oxidation products from unoxidized polyunsaturated fatty acids and consequently inhibited their further breakdown into TBARS. Intriguingly, the QS emulsion exhibited poor physical stability, characterized by oiling-off at 21 days and the highest TSI value. However, it contained lower concentrations of oxidation products, which possibly be attributed to its intrinsic antioxidant components.

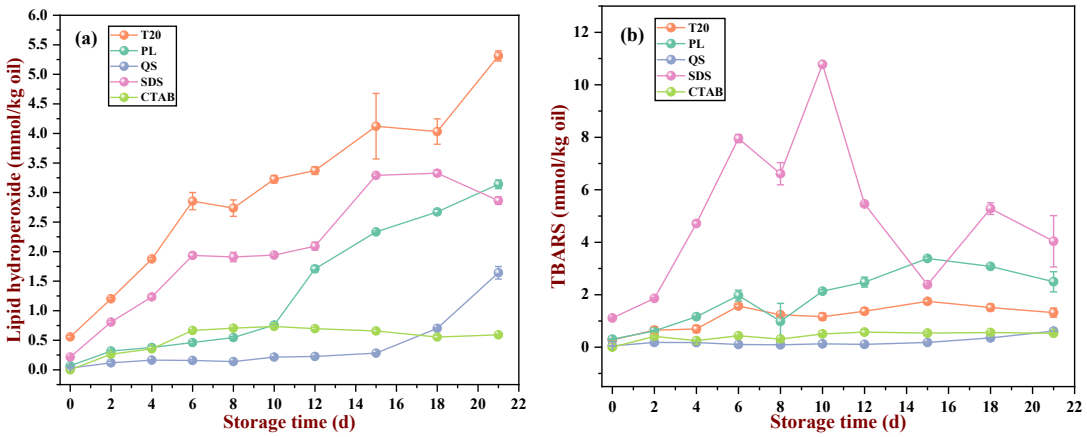


Fig. 3 Time-dependent changes in LOOH (a) and TBARS (b) concentrations in SFO-emulsions during the entire storage period.

3.3 Micelle Particle Size and TG Content in Emulsion Aqueous Phase

Cryo-TEM and DLS techniques were employed to examine the microstructure and particle sizes of the emulsion aqueous phase (**Fig. 4a** and **4b**). Following high-speed

centrifugation, the aqueous phase beneath the emulsified layer appeared translucent. This aqueous phase contained micelles and swollen micelles (containing a certain amount of TG). **Fig. 4b** revealed that SDS and CTAB generated the initial aqueous phase smallest sizes, approximating 55-56 nm. It indicated that these two surfactants were more prone to form smaller micellar particles, corresponding to emulsions containing the smallest D [3,2]. In contrast, the larger initial micellar sizes in T20 and QS emulsions aqueous phases (64.21 nm and 58.05 nm) were observed. By the end of storage, the aqueous micellar size for T20 and QS increased to 66.53 and 62.33 nm, respectively. Interestingly, the particle size for PL surged from 52.35 to 88.38 nm throughout storage, suggesting that coalescence events might occur among the micelles in the aqueous phase[34].

Monitoring the fluctuations in TG content within aqueous phase micelles during storage revealed obvious differences across the varying surfactant systems (**Fig. 4c**). Initially, the aqueous phases of SDS and CTAB presented the highest TG contents (~28 mmol/L). Because these two surfactants tend to form uniform small colloidal particles, more of these small colloids remained in the aqueous phase following high-speed centrifugation, leading to highest TG concentrations in the aqueous phase. This content remained almost unchanged during storage, indicating sufficient surfactant in the aqueous system to stabilize the small colloids, thereby retaining them in the aqueous phase. The T20 aqueous phase retained approximately 17 mmol/L of TG, which fluctuated slightly during storage but showed no significant change. The initial TG contents in the aqueous phases of QS and PL were similar, decreasing from 7.29 and 8.03 mmol/L to 4.8 and 2.36 mmol/L, respectively, over the storage period. Notably, the TG content in the PL system decreased sharply to 2.87 mmol/L at day 4 of storage-a reduction of 64.26%-before entering a phase of slow decline. This decrease in TG might be due to Ostwald ripening or coalescence, forming larger particles that enter the upper oil phase during centrifugation[34].

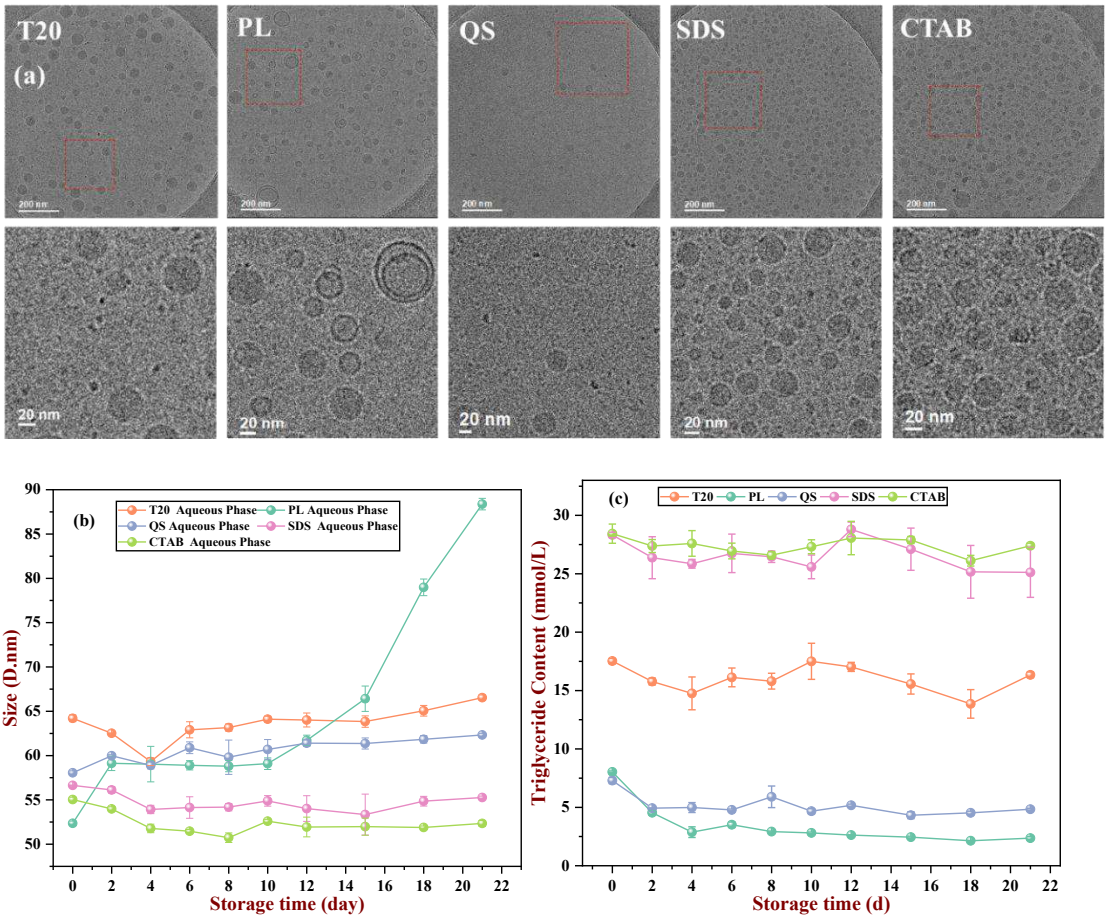


Fig. 4 Cryo-TEM micrographs of the emulsion aqueous phase micelles (a); the changes in particle size of micelles in aqueous phase (b); and variation in TG content of aqueous-phase micelles during storage (c).

3.4 LOOH and MDA Contents in Emulsion Aqueous Phase

The mass transport effects of different surfactant micelles were investigated by monitoring aqueous phase oxidation product levels throughout storage. **Fig. 5a** demonstrated that the temporal profile of LOOH generation in the aqueous phase paralleled that of total LOOH. After being generated in the oil phase, LOOH migrated into the aqueous phase and there combined with surfactants to form mixed micelles. The LOOH contents in the aqueous phases of PL and QS surged on days 12 and 16, respectively, consistent with the surge in overall emulsion LOOH content. The MDA content across the different emulsion aqueous phases followed the order: SDS > CTAB > T20 > QS > PL (**Fig.5b**). The CTAB emulsion and aqueous phase globally possessed lower LOOH and TBARS values (2.85 μmol/L). However, the sharp increase of MDA

in its aqueous phase suggested that compared to LOOH, CTAB aqueous micelles were more inclined to transport the generated MDA to the aqueous phase, which might be related to the formed interfacial structure. During the early storage of PL, the decrease in aqueous MDA concentration was possibly due to the sharp decrease in initial TG content. The moderate MDA levels observed for T20 indicated that T20 micelles transported LOOH to the aqueous phase, migrating it away from the oxidation site and thus delaying the further degradation of LOOH.

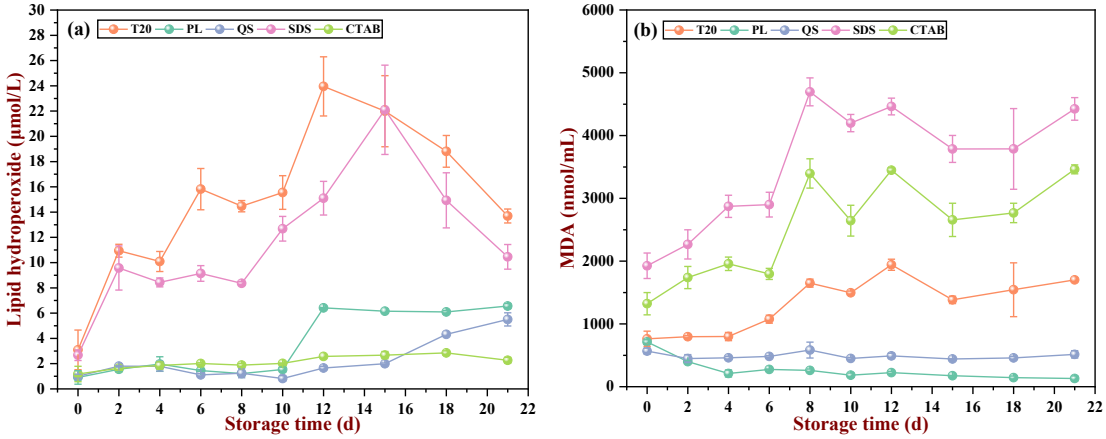


Fig. 5 Production of LOOH (a) and MDA (b) in the emulsion aqueous phase as a function of storage time.

3.5 Dynamic Interfacial Tension

Surfactants exert a critical influence on emulsion formation and stabilization through their interfacial activity. Low interfacial tension values are known to promote emulsification, as the energy required to disrupt the interface and thereby generate small, stable droplets is reduced. Nevertheless, the dynamic equilibrium of interfacial adsorption largely governs this process[23]. As illustrated in **Fig. 6**, the capacity to lower interfacial tension varies markedly among different emulsifiers. All samples showed a similar decreasing trend over time, and the final interfacial tension values decreased in the following order: PL > SDS > QS > T20 > CTAB. With the exception of PL, the remaining four surfactants showed rapid adsorption at the oil-water interface. Their interfacial tension decreased sharply during the first 1000 s, followed by a slower decline over a longer period until a plateau was reached. For the QS sample, the

interfacial tension fell from 30.65 to 10.99 mN/m within the initial 1000 s. PL reached adsorption dynamic equilibrium at 2500 s, with the interfacial tension decreasing from 40.40 to 24.47 mN/m. These results aligned with previously reported findings, where the interfacial tension of a soy lecithin- corn oil was about 25 mN/m, while that of the saponin-corn oil system was 6 mN/m[35]. Reducing interfacial tension might be a favorable factor for emulsion stability, but it was not the decisive factor[36]. The interfacial film properties resulting from surfactant adsorption also significantly affected emulsion stability.

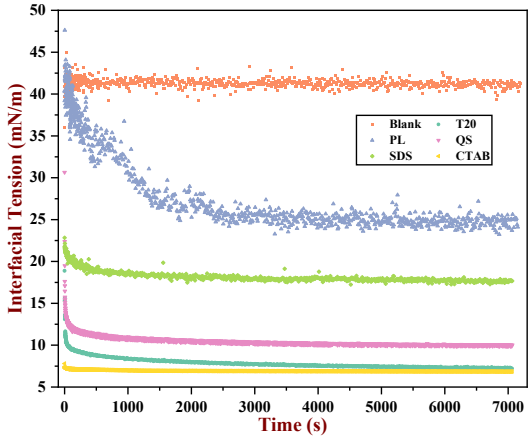


Fig. 6 Time-dependent interfacial tension (DIFT) of flaxseed oil in different surfactant systems.

3.6 Emulsion Interfacial Film Properties

The interfacial characteristics of O/W emulsions prepared with various surfactants were investigated using the EPR spin probe method. 5-DSA, a spin-labeled fatty acid analogue consisting of stearic acid with an N-O• group at the C-5 position of its alkyl chain, was employed as the probe. Owing to its amphiphilic character, 5-DSA tends to situate preferentially at the oil-water interface, where it interacts with surfactant molecules[18,37]. The 5-DSA spin probe molecule can serve as an effective tool for elucidating molecular organization and dynamic changes at the oil-water interface in heterogeneous systems[18,38-40]. The EPR spectrum of the nitroxide spin probe 5-DSA (Fig. 7) shows a triplet caused by hyperfine coupling of the nitrogen nuclear spin (I = 1) with the unpaired electron spin (S = 1/2)[17]. Theoretically, 5-DSA forms three narrow

peaks of almost identical intensity in solution, while the appearance of different heights and widths in **Fig. 7** indicates that the probe had restricted motion in the environment.

To quantitatively assess probe mobility and interfacial rigidity, the EPR spectra were processed using the EasySpin simulation model, yielding τ_R and S (**Table 1**). A decrease in 5-DSA mobility leads to a higher τ_R, indicating increased microviscosity around the spin probe. Similarly, a rise in S reflects greater interfacial rigidity. Additionally, the isotropic hyperfine splitting constant (α_0'), derived from the EPR data, provides information on the micropolarity surrounding the probe[21]. QS and PL had higher τ_R values, 1.25 and 1.07 ns respectively, indicating that the microenvironment near the rotational probe in both emulsions was relatively viscous. This behavior was attributed to the distinct molecular structures. Phospholipids possessed two hydrophobic tails and a zwitterionic polar head group, whereas QS comprised hydrophobic regions (quillaic acid) along with hydrophilic sugar or acyl residues (e.g., rhamnose, xylose, arabinose, galactose, fructose, and glucuronic acid). Consequently, the wobbling motion of the probe at the interface was restricted [17]. In the SDS- and CTAB-stabilized emulsions, the 5-DSA probe exhibited lower τ_R values (0.61 ns and 0.49 ns, respectively), indicating high probe mobility within the microenvironment, low local viscosity, and the formation of emulsions with lower interfacial rigidity (S = 0.09). In emulsions characterized by such low-viscosity, mass transport between phases was possibly accelerated. The higher S value for T20 (S=0.13) suggested the formation of a rigid surfactant monolayer. SDS and CTAB formed low-viscosity, low- rigidity films with good interfacial fluidity, leading to rapid mass exchange in the emulsions. The high-viscosity, high-polarity interfacial films of QS, PL, and T20 (high α_0' value) might affect reactant diffusion. Therefore, the MDA in the aqueous phases of QS, PL and T20 was lower than that of SDS and CTAB. Although T20 formed a rigid interface (exhibiting the highest S value), it lacked a charge-based protective mechanism. The oxidation occurred rapidly, indicating that despite the ordered nature of its interfacial film, it was unable to effectively block free radical attacks or inhibit metal ion

penetration. In conclusion, EPR spectroscopy results demonstrated that O/W emulsions prepared using T20, QS, PL, SDS, and CTAB presented emulsions with different local viscosities, polarities, and surfactant-stabilized films.

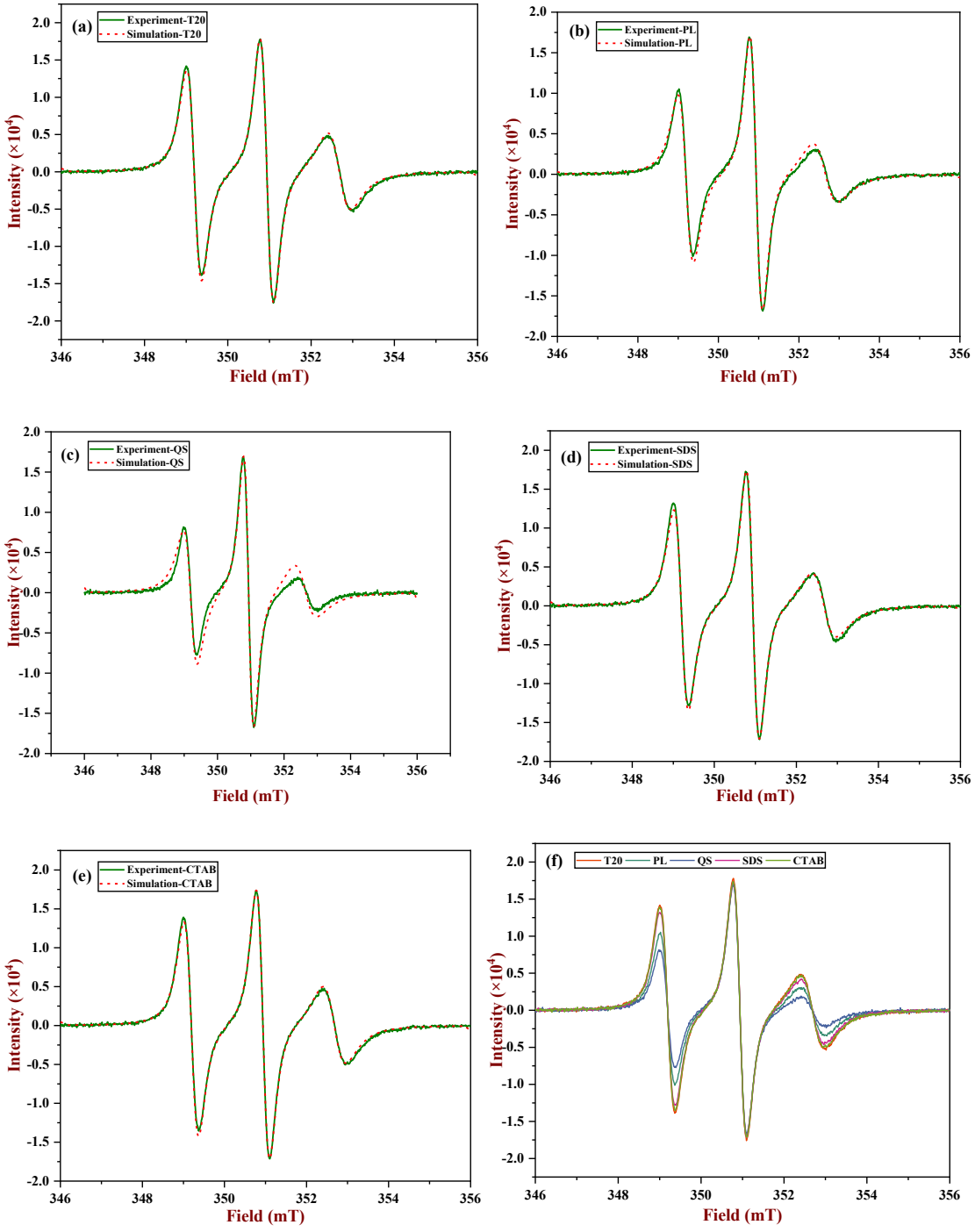


Fig. 7 Experimental and simulated EPR spectra of the 5-DSA spin probe in various emulsions.

Table 1 Rotational correlation time (τ_R), order parameter (S) and isotropic hyperfine

splitting constant(α_0') of 5-DSA in variously formulated O/W emulsions.

	τ_R（ns）	S	α_0'(G)
T20	0.80±0.04	0.13±0.01	17.5±0.1
PL	1.07±0.09	0.11±0.01	17.5±0.1
QS	1.25±0.09	0.12±0.02	17.6±0.1
SDS	0.61±0.03	0.09±0.01	17.4±0.1
CTAB	0.49±0.03	0.09±0.01	17.4±0.1

4 Conclusion

In this study, emulsions were prepared using various surfactant molecules (T20, SDS, CTAB, QS, and PL). The overall emulsion stability and the mass transport of oxidation products by aqueous-phase micelles were monitored to elucidate the stability mechanism across the oil, aqueous, micelle phases, and the interface. The results revealed that during storage, SDS and CTAB had lower TSI values (<1.5), exhibiting better physical stability. PL and QS formed high-viscosity, high-polarity interfacial films that restricted reactant diffusion, resulting in lower oxidation product contents in the aqueous phase. Conversely, the interfacial films formed by SDS and CTAB had high fluidity, promoting mass transport, wherein CTAB micelles were more inclined to migrate the smaller molar mass secondary oxidation product MDA. Notably, T20 delayed the generation of TBARS, which increased only slowly from 0.28 to 1.32 mmol/kg oil, by facilitating the transport of LOOH to the aqueous phase, thereby removing them from the oxidation site. From a physical structure perspective, this study reveals the mechanism by which surfactant types influence micellar mass transport and interfacial properties to regulate the emulsion oxidation process, providing an important basis for designing emulsion systems that balance both physical and chemical stability.

Author Contributions

Xintian Wang: Writing – review & editing, Writing – original draft, Formal analysis, Data curation. **Hongjian Chen**: Writing – original draft; Investigation.**Qian Zhang**: Data curation; Formal analysis; Methodology. **Xingfang Xiao**: Data curation; Investigation; Methodology. **Alejandro Cifuentese**: Investigation; Writing-original

draft. **Elena Ibanezde**: Data curation; Investigation. **Bifeng Liu**: Data curation; Investigation. **Peiwu Li**: Data curation; Investigation; Methodology. **Zhaowei Zhang:** Writing – review & editing, Writing – original draft; Investigation. **Qianchun Deng**: Conceptualization; Funding acquisition; Project administration; Resources; Supervision; Writing-original draft; Writing-review and editing.

Conflicts of Interest

There are no conflicts to declare.

Acknowledgements

The authors gratefully acknowledge financial support from the Earmarked Fund for China Agriculture Research System (CARS-14), the Innovation Group Project of Hubei Province (2023AFA042), and the Science and Technology Projects of Xizang Autonomous Region (XZ202502ZY0068).

References

1 Laguerre, M., Bily, A., Roller, M. & Birtic, S. Mass Transport Phenomena in Lipid Oxidation and Antioxidation. *Annual Review of Food Science and Technology, Vol 8* **8**, 391-411 (2017). https://doi.org/10.1146/annurev-food-030216-025812

2 villeneuve, P. *et al.* Lipid oxidation in emulsions and bulk oils: a review of the importance of micelles. *Critical Reviews in Food Science and Nutrition* **63**, 4687-4727 (2023). https://doi.org/10.1080/10408398.2021.2006138

3 Laguerre, M. *et al.* What Makes Good Antioxidants in Lipid-Based Systems? The Next Theories Beyond the Polar Paradox. *Critical Reviews in Food Science and Nutrition* **55**, 183-201 (2014). https://doi.org/10.1080/10408398.2011.650335

4 Villeneuve, P., Durand, E. & Decker, E. A. The Need for a New Step in the Study of Lipid Oxidation in Heterophasic Systems. *Journal of Agricultural and Food Chemistry* **66**, 8433-8434 (2018). https://doi.org/10.1021/acs.jafc.8b03603

5 Wang, X. T. *et al.* Recent advances in understanding the interfacial activity of antioxidants in association colloids in bulk oil. *Advances in Colloid and Interface Science* **325**, 103117 (2024). https://doi.org/10.1016/j.cis.2024.103117

6 Wang, X. *et al.* Regulation of Microlocalization of Antioxidants by Surfactant Micelles in Oil-in-Water Emulsions. *Journal of Agricultural and Food Chemistry* **72**, 25306-25318 (2024). https://doi.org/10.1021/acs.jafc.4c08855

7 Wang, X., Chen, H., Xu, Y. & Deng, Q. The role of micro-structures in the aqueous phase of emulsion in lipid oxidation process. *Food Chem.* **464** (2025). https://doi.org/10.1016/j.foodchem.2024.141760

8 Durand, E., Troncho, T., Koli, H., Robichon, C. & Villeneuve, P. Focus on the role of mixed micelles and lipid droplets in the oxidative stability of oil-in-water emulsions using size distribution Taylor dispersion analysis. *Curr Res Food Sci*

12, 101369 (2026). https://doi.org/10.1016/j.crfs.2026.101369

9 Durand, E., Troncho, T. & Villeneuve, P. Evaluation of antioxidant-surfactant interactions using size distribution Taylor dispersion analysis: measuring antioxidant partitioning and size of native-state micelles. *Curr Res Food Sci* **11**, 101142 (2025). https://doi.org/10.1016/j.crfs.2025.101142

10 Wang, X. *et al.* Association colloids in flaxseed oil: Supramolecular platforms for targeted antioxidant delivery. *Food Research International* **225** (2026). https://doi.org/10.1016/j.foodres.2025.118022

11 Wang, X. *et al.* Effect of sesamol on the physical and chemical stability of plant-based flaxseed oil-in-water emulsions stabilized by proteins or phospholipids. *Food & Function* **12**, 2090-2101 (2021). https://doi.org/10.1039/d0fo02420a

12 Gharibzahedi, S. M. T., Razavi, S. H. & Mousavi, S. M. Ultrasound-assisted formation of the canthaxanthin emulsions stabilized by arabic and xanthan gums. *Carbohydrate Polymers* **96**, 21-30 (2013). https://doi.org/10.1016/j.carbpol.2013.03.085

13 Chen, F. *et al.* Inhibition of lipid oxidation in nanoemulsions and filled microgels fortified with omega-3 fatty acids using casein as a natural antioxidant. *Food Hydrocolloids* **63**, 240-248 (2017). https://doi.org/10.1016/j.foodhyd.2016.09.001

14 Cheng, C. *et al.* Effect of flaxseed polyphenols on physical stability and oxidative stability of flaxseed oil-in-water nanoemulsions. *Food Chem.* **301**, 125207 (2019). https://doi.org/10.1016/j.foodchem.2019.125207

15 Steffes, V. M., Zhang, Z. N., Ewert, K. K. & Safinya, C. R. Cryo-TEM Reveals the Influence of Multivalent Charge and PEGylation on Shape Transitions in Fluid Lipid Assemblies: From Vesicles to Discs, Rods, and Spheres. *Langmuir* **39**, 18424-18436 (2023). https://doi.org/10.1021/acs.langmuir.3c02664

16 Joshi, M. *et al.* Interfacial and emulsifying properties of lentil protein isolate. *Food Chem* **134**, 1343-1353 (2012). https://doi.org/10.1016/j.foodchem.2012.03.029

17 Demisli, S. *et al.* Structure, activity and dynamics of extra virgin olive oil-in-water nanoemulsions loaded with vitamin D3 and calcium citrate. *Journal of Molecular Liquids* **306**, 112908 (2020). https://doi.org/10.1016/j.molliq.2020.112908

18 Golfomitsou, I., Mitsou, E., Xenakis, A. & Papadimitriou, V. Development of food grade O/W nanoemulsions as carriers of vitamin D for the fortification of emulsion based food matrices: A structural and activity study. *Journal of Molecular Liquids* **268**, 734-742 (2018). https://doi.org/10.1016/j.molliq.2018.07.109

19 Savić, V. *et al.* Tacrolimus loaded biocompatible lecithin-based microemulsions with improved skin penetration: Structure characterization and in vitro/in vivo performances. *International Journal of Pharmaceutics* **529**, 491-505 (2017). https://doi.org/10.1016/j.ijpharm.2017.07.036

20 Papadimitriou, V. *et al.* Biocompatible microemulsions based on limonene: Formulation, structure, and applications. *Langmuir* **24**, 3380-3386 (2008). https://doi.org/10.1021/la703682c

21 Avramiotis, S. *et al.* Lecithin organogels used as bioactive compounds carriers. A

microdomain properties investigation. *Langmuir* **23**, 4438-4447 (2007). https://doi.org/10.1021/la0634995

22 Amine, C., Dreher, J., Helgason, T. & Tadros, T. Investigation of emulsifying properties and emulsion stability of plant and milk proteins using interfacial tension and interfacial elasticity. *Food Hydrocolloids* **39**, 180-186 (2014). https://doi.org/10.1016/j.foodhyd.2014.01.001

23 Kalogianni, E. P. *et al.* A multi-probe non-intrusive electrical technique for monitoring emulsification of hexane-in-water with the emulsifier CE soluble in both phases. *Colloids and Surfaces a-Physicochemical and Engineering Aspects* **354**, 353-363 (2010). https://doi.org/10.1016/j.colsurfa.2009.09.004

24 Jeong, S. J., Kim, S., Echeverria-Jaramillo, E. & Shin, W. S. Effect of the emulsifier type on the physicochemical stability and in vitro digestibility of a lutein/zeaxanthin-enriched emulsion. *Food Science and Biotechnology* **30**, 1509-1518 (2021). https://doi.org/10.1007/s10068-021-00987-9

25 Züge, L. C. B., Maieves, H. A., Silveira, J. L. M., Silva, V. R. d. & Scheer, A. d. P. Use of avocado phospholipids as emulsifier. *LWT - Food Science and Technology* **79**, 42-51 (2017). https://doi.org/10.1016/j.lwt.2017.01.013

26 Cardenia, V., Waraho, T., Rodriguez-Estrada, M. T., Julian McClements, D. & Decker, E. A. Antioxidant and Prooxidant Activity Behavior of Phospholipids in Stripped Soybean Oil-in-Water Emulsions. *Journal of the American Oil Chemists' Society* **88**, 1409-1416 (2011). https://doi.org/10.1007/s11746-011-1807-y

27 Mosca, M., Ceglie, A. & Ambrosone, L. Effect of membrane composition on lipid oxidation in liposomes. *Chemistry and Physics of Lipids* **164**, 158-165 (2011). https://doi.org/10.1016/j.chemphyslip.2010.12.006

28 Wang, L. *et al.* Effects of tocopherols on the stability of flaxseed oil-in-water emulsions stabilized by different emulsifiers: Interfacial partitioning and interaction. *Food Chem.* **374**, 131691 (2022). https://doi.org/10.1016/j.foodchem.2021.131691

29 Liang, L. *et al.* Physical and Oxidative Stability of Flaxseed Oil-in-Water Emulsions Fabricated from Sunflower Lecithins: Impact of Blending Lecithins with Different Phospholipid Profiles. *Journal of Agricultural and Food Chemistry* **65**, 4755-4765 (2017). https://doi.org/10.1021/acs.jafc.7b01469

30 Llinares, R., Ramírez, P., Carmona, J., Carrillo, F. & Munñoz, J. Formulation and optimization of emulsions based on bitter fennel essential oil and EO/BO block copolymer surfactant. *Colloids and Surfaces A: Physicochemical and Engineering Aspects* **536**, 142-147 (2018). https://doi.org/10.1016/j.colsurfa.2017.07.027

31 Zhao, X. *et al.* Eco-Friendly Pickering Emulsion Stabilized by Silica Nanoparticles Dispersed with High-Molecular-Weight Amphiphilic Alginate Derivatives. *ACS Sustainable Chemistry & Engineering* **6**, 4105-4114 (2018). https://doi.org/10.1021/acssuschemeng.7b04508

32 Ji, Y. *et al.* Study on shearing resistance and the stability of O/W emulsion of the inclusive and hydrophobic association systems by activation energy methodology.

Journal of Polymer Research **21** (2014). https://doi.org/10.1007/s10965-014-0517-1

33 Ji, Y., Kang, W., Meng, L., Hu, L. & Yang, H. Study of the solution behavior of β-cyclodextrin amphiphilic polymer inclusion complex and the stability of its O/W emulsion. *Colloids and Surfaces A: Physicochemical and Engineering Aspects* **453**, 117-124 (2014). https://doi.org/10.1016/j.colsurfa.2014.04.016

34 Klooster, S. t. *et al.* Tiny, yet impactful: Detection and oxidative stability of very small oil droplets in surfactant-stabilized emulsions. *Journal of Colloid and Interface Science* **652**, 1994-2004 (2023). https://doi.org/10.1016/j.jcis.2023.09.005

35 Bai, L., Huan, S., Gu, J. & McClements, D. J. Fabrication of oil-in-water nanoemulsions by dual-channel microfluidization using natural emulsifiers: Saponins, phospholipids, proteins, and polysaccharides. *Food Hydrocolloids* **61**, 703-711 (2016). https://doi.org/10.1016/j.foodhyd.2016.06.035

36 Gu, L. *et al.* Protection of beta-carotene from chemical degradation in emulsion-based delivery systems using antioxidant interfacial complexes: Catechin-egg white protein conjugates. *Food Res Int* **96**, 84-93 (2017). https://doi.org/10.1016/j.foodres.2017.03.015

37 Papadimitriou, V., Sotiroudis, T. G. & Xenakis, A. Olive oil microemulsions: Enzymatic activities and structural characteristics. *Langmuir* **23**, 2071-2077 (2007). https://doi.org/10.1021/la062608c

38 Kalogianni, E. P. *et al.* Effect of oleic acid on the properties of protein adsorbed layers at water/oil interfaces: An EPR study combined with dynamic interfacial tension measurements. *Colloids and Surfaces B-Biointerfaces* **158**, 498-506 (2017). https://doi.org/10.1016/j.colsurfb.2017.07.022

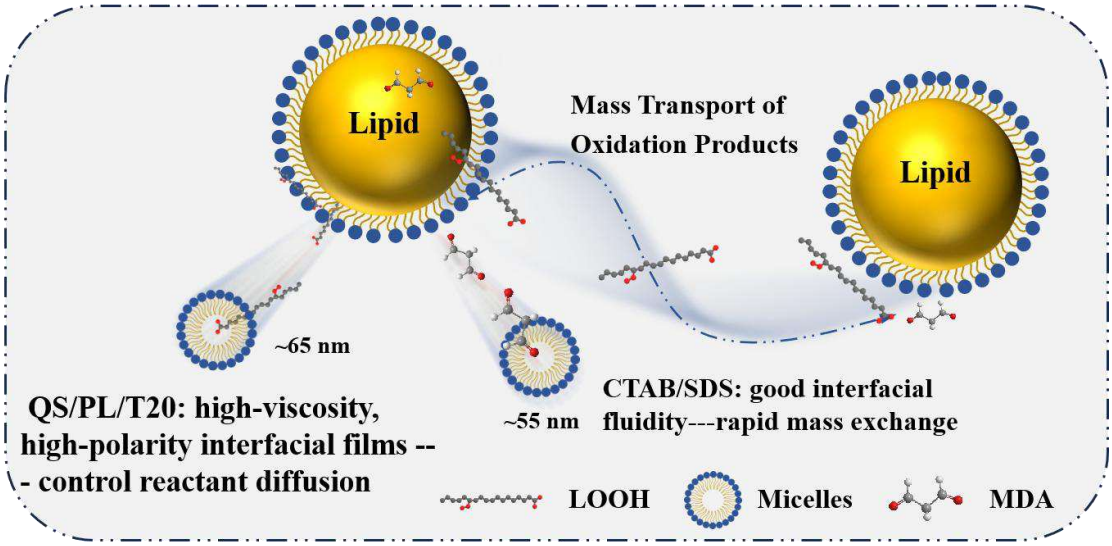
39 Sergeev, A. *et al.* EPR and NMR study of molecular components mobility and organization in goat milk under ultrasound treatment. *Ultrasonics Sonochemistry* **77**, 105673 (2021). https://doi.org/10.1016/j.ultsonch.2021.105673

40 Mitsou, E. *et al.* Hydroxytyrosol encapsulated in biocompatible water-in-oil microemulsions: How the structure affects absorption. *Colloids and Surfaces B-Biointerfaces* **184**, 110482 (2019). https://doi.org/10.1016/j.colsurfb.2019.110482

Highlights

- Interfacial structures govern micelle-driven mass transports in emulsions.
- Viscous PL and QS interfaces restricted the diffusion of oxidation products.
- Fluid SDS and CTAB interfaces accelerated micelle-mediated mass transport.
- T20 micelles partitioned LOOH into the aqueous phase, delaying TBARS formation.

582 **TOC**


Lipid
Mass Transport of
Oxidation Products
Lipid
~65 nm
~55 nm
QS/PL/T20: high-viscosity,
high-polarity interfacial films --
- control reactant diffusion
CTAB/SDS: good interfacial
fluidity---rapid mass exchange
LOOH
Micelles
MDA

583